Results in Engineering 23 (2024) 102456

Contents lists available at ScienceDirect

Results in Engineering

journal homepage: www.sciencedirect.com/journal/results-in-engineering

Techno-economic assessment of solar photovoltaic electrification and calcium looping technology as decarbonisation pathways of alumina industry

Javier Sáez-Guinoa [a,b], Inés Senante [b], Eva Llera-Sastresa [b], Luis M. Romeo [a,b,*]

[a] Aragon Institute for Engineering Research (i3A). Campus Río Ebro I+D+i, Mariano Esquillor s/n, 50018, Zaragoza, Spain
[b] School of Engineering and Architecture. University of Zaragoza, Campus Río Ebro, María de Luna 3, 50018, Zaragoza, Spain

ARTICLE INFO

Keywords:
Alumina
Decarbonisation
CO_2 capture
Electrification
Calcium looping
Techno-economics
Solar photovoltaic

ABSTRACT

Aluminium industry stands out as a significant source of CO_2 emissions, due partially to the high energy demand of the alumina extraction stage. Accordingly, this study explores the implementation of direct resistive heating of mid-temperature processes in alumina production as an alternative to decrease CO_2 emissions. Additionally, two different strategies are evaluated to decarbonize alumina industry: the generation of renewable electricity through solar photovoltaic panels and the integration of a CO_2 capture plant based on calcium looping technology. This work comprehends the modelling and sizing of these plants and the assessment of their economic performance through the calculation of their Net Present Value and their respective payback periods. The integration of both strategies into an alumina refinery model reveals that electrification of low and mid-temperature processes yields a 15 % reduction in CO_2 direct emissions, whereas calcium looping demonstrates the potential to capture 97 % of emissions with a 7 % energy penalty. Also, economic assessments indicate substantial potential for improvement through in-site electricity generation via solar photovoltaic panels, exhibiting a payback time of 4.5 years. Conversely, the feasibility of a calcium-looping plant is hindered by high capital expenses, necessitating a longer payback period of 19–24 years. Sensitivity analyses underscore the suitability of in-site renewable electricity generation, whereas carbon emission taxes emerge as crucial in incentivizing carbon-neutral processes, with thresholds around 95–125 €/tonne of CO_2. Despite potential deviations from real industrial settings, this study provides evidence for environmentally friendly strategies in alumina production that demonstrate limited adverse effects on economic performance.

Abbreviations

CCS	Carbon capture and storage	N_{cycles}	Number of carbonation-calcination cycles
CaL	Calcium looping	X_N	Carbonation conversion ratio of a single CaO particle
CaO	Calcium oxide	r_N	Percentage of CaO particles gone through N_{cycles}
NPV	Net present value	k	Sorption decay constant
PV	Solar photovoltaic	X_r	Residual sorption activity
PSH	Peak sun hours	F_{CaCO3}	Molar flowrate of fresh $CaCO_3$ entering the calciner
N	Number of PV panels	F_{CaO}	Molar flowrate of purged CaO leaving the calciner
E	Electricity demand	PB	Payback time
A	Amperage	V_T	Cashflow after taxes
V	Voltage	t	Time period
γ	Efficiency of PV panels	I_0	Initial capital investments
L	Land occupation	i	Discount rate
X_{ave}	Average carbonation conversion ratio of circulating CaO	V_0	Cashflow after taxes of base cases

(continued on next column)

(continued)

1. Introduction

The European Union has established as a priority to achieve carbon neutrality by the year 2050. This ambitious objective needs the implementation of comprehensive decarbonisation strategies within the

* Corresponding author. Aragon Institute for Engineering Research (i3A). Campus Río Ebro I+D+i, Mariano Esquillor s/n, 50018, Zaragoza, Spain.
E-mail address: luismi@unizar.es (L.M. Romeo).

https://doi.org/10.1016/j.rineng.2024.102456
Received 26 March 2024; Received in revised form 14 June 2024; Accepted 20 June 2024
Available online 21 June 2024

industrial sector, responsible of emitting approximately 24 % of CO_2 global emissions [1]. Most of these industrial emissions originate from the use of fossil fuels in processes characterized by elevated energy consumption levels.

A significant industrial process in this regard is aluminium production. Aluminium industry was estimated to be the source of emitting nearly 270 million tonnes of direct CO_2 in 2022 [2], as a consequence of its high energy utilization. The gross energy requirement of the whole primary aluminium production chain is estimated at 210 ± 10 GJ per tonne of aluminium [3]. This energy consumption occurs mainly in two different stages of aluminium production process: the extraction of alumina from bauxite ore (Bayer process) and the smelting reduction of alumina to produce aluminium (Hall-Héroult process) [4].

Alumina extraction is commonly carried out via Bayer process, in which bauxite is digested in a NaOH solution to isolate the aluminium content of the mineral. Then, aluminium hydroxide is precipitated and subsequently calcined at high temperatures (>1,000 °C) to obtain smelter grade alumina. Afterwards, alumina is reduced in a smelting plant using carbon anodes and electricity via Hall-Héroult process. Pure aluminium is obtained, which is finally casted in-site to produce aluminium ingots. A simplified flowsheet of the primary aluminium production route is shown in Fig. 1.

Thermal energy demand of Bayer process, necessary for the digestion of the ore and the hydroxide calcination, is estimated on world average at 10,225 MJ per tonne of alumina [5], though composition and quality of bauxite can induce remarkable differences on this value [6]. Considering that nearly 2 tonnes of alumina are needed for the production of 1 tonne of aluminium, energy intensity of alumina production is approximately 20,450 MJ per tonne of aluminium. Moreover, electricity demand of Hall-Héroult process is estimated at 50,770 MJ per tonne of aluminium [7]. Hence, primary aluminium production stands out as a high energy-intensive metal [8]. Thus, efforts must be made to decarbonize this industry and minimize their CO_2 emissions.

Numerous studies confirm that the utilization of renewable electricity in the Hall-Héroult process is essential for minimizing environmental impacts and attaining carbon-neutral aluminium production [9–11]. However, it does not exist a unique clear pathway to decarbonize alumina industry and mitigate CO_2 emissions from Bayer process stage. Efforts are focused on valorisation or avoidance of bauxite residues (known as *redmuds* because of its iron composition) via iron smelting prior to caustic digestion [12], via a two-stage digestion [13], a reductive digestion [14] or a calcification-carbonation method [15]. The smart management of tailings of bauxite residues results crucial to control its environmental impacts [16]. However, most of these approaches do not solve the problem of carbon emissions, but increase energy consumption and lack economic viability [17].

Other strategies under development to decarbonize industrial sector include the substitution of fossil fuels with biomass-based fuels [18], the electrification of the industry through green hydrogen combustion or direct resistive heating [19] and the implementation of carbon capture and storage (CCS) technologies [20]. In reference to alumina industry, companies are currently testing the large-scale viability of some of these technologies. Worsley Alumina Pty Ltd tested the feasibility of using biomass by adding 30 % load of waste from pine logging in a multi-fuel boiler [21], resulting in the abatement of approximately 5.75 kt of equivalent CO_2 emissions. Norsk Hydro ASA completed successfully the industrial-scale production of recycled aluminium with the use of green hydrogen in substitution of natural gas combustion [22]. Rio Tinto Group and Sumitomo Corporation are also planning the construction of a hydrogen plant to test its utilization during alumina calcination process, which is expected to be in operation in 2025 [23].

With regards to direct electrification, Alcoa Corporation is also testing the use of direct resistive heating in alumina production facilities, aiming to achieve carbon neutrality. The electric calcination is being piloted at Pinjarra refinery [24] whereas research on low-temperature digestion and evaporation processes is being developed through Mechanical Vapour Recompression [25]. Hydro Alunorte SA installed also in 2022 a 60 MW electric boiler to reduce coal-fired power demand of its alumina refinery [2]. Aughinish Alumina Ltd is also facing the development of high-pressure electric boilers to replace gas-fired boilers, with the aim of reducing by 10 % their CO_2 emissions [26]. The elevated amounts of energy required for alumina refinement plants hamper a wider implementation of direct electrification.

CCS strategies are currently an efficient alternative to reduce the effects of CO_2 emitted in power plants [27] or in other significant CO_2 emitter industries [28]. However, CCS technologies are yet under development in aluminium industry. Aluminium Dunkerque and Norsk Hydro ASA have both announced that they are exploring options to use CCS technologies for minimizing aluminium smelting emissions [2]. However, no industrial projects are currently found regarding alumina production. In literature research, a study proposed a conventional amine-based carbon capture system for CO_2 emissions from alumina refinement [29]. Results indicated that a 65.29 % reduction of direct CO_2 emissions was achieved with respect to conventional aluminium ingot production. Another study proposed the integration of a calcium-looping (CaL) plant to capture and store CO_2 emissions from alumina production [30]. Results showed a 7 % penalty of energy consumption for the avoidance of 95 % of CO_2 emissions, resulting an efficient alternative that couples both environmental and economic aspects.

CaL is a promising technology in CCS systems because of its relatively low energy penalty in highly integrated systems [31]. CaL system consists of putting the flue gases containing CO_2 through a carbonation-calcination cycle. Calcium oxide (CaO) is used as a sorbent, producing calcium carbonate, which is later decomposed in a calciner. A basic flowsheet of a CaL configuration is shown in Fig. 2. Among other limitations of this technology, such as the need of generating oxygen for the oxy-fuel combustion in the calciner, a main drawback is the sorption capacity decay that CaO suffers with each cycle of carbonation and calcination [32]. To overcome this and get a suitable conversion of the carbonation reaction, a fraction of CaO must be purged and fresh $CaCO_3$ must be introduced in the loop [33]. The use of CaO in bauxite digestion can involve a synergy between CaL and alumina industry, using purged CaO as desilication agent in Bayer process.

Considering all previous studies mentioned above and the current state of the art, this work aims to assess the techno-economic feasibility of an alumina refinery that achieves carbon neutrality and zero CO_2 emissions. For this purpose, two different technologies are proposed in the study: (i) the implementation of solar photovoltaic panels for the electrification of low and mid-temperature stages of Bayer process, and

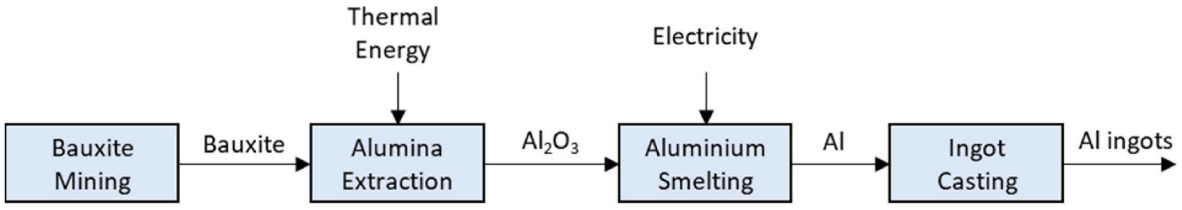

Fig. 1. Most common industrial route of aluminium production.

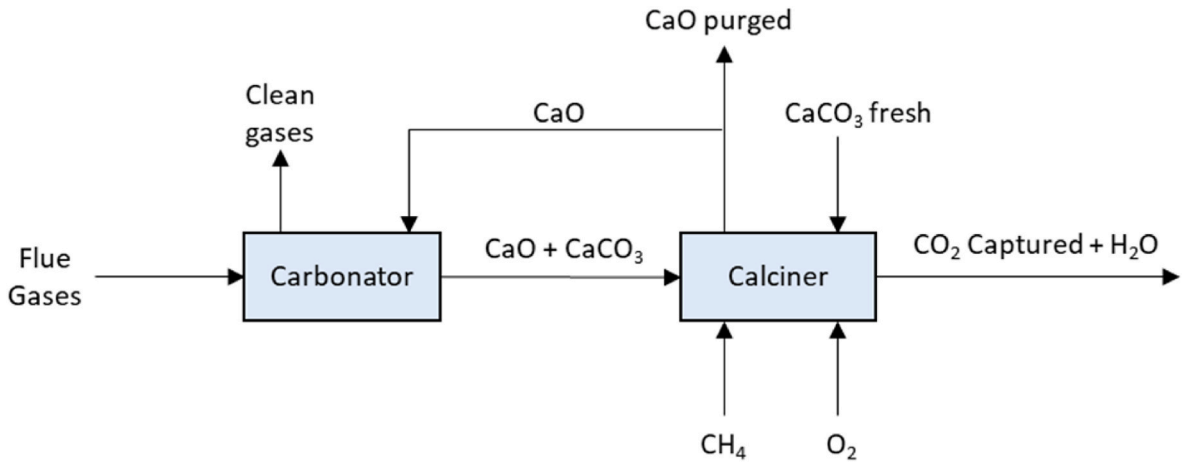

Fig. 2. Simplified flowsheet of a calcium looping plant.

(ii) the modelling of a calcium-looping plant to capture and store post-combusted CO_2 from the calcination stage. The simulation and optimization of different integration proposals is presented and techno-economic assessments are discussed based on Net Present Value (NPV) and payback time estimations.

2. Materials and methods

The study comprehends the modelling of an alumina refinery and different alternatives of decarbonisation, that include the production of necessary renewable electricity through solar photovoltaic panels (PV) and the implementation of a CaL plant to capture post-combusted CO_2. For comparison purposes, the external purchase of grid electricity is considered in base cases (S100, S200 and S400), in which PV and/or CaL are not implemented. Different levels of electrification temperatures are also proposed in the work to analyse the changes in energy requirements of the complete system. The different case studies considered in the work are shown in Table 1. For each of the three different electrification levels that are studied, four different layouts are proposed: (i) the base case of a single alumina production plant, (ii) the addition of a PV plant to generate renewable electricity, (iii) the integration of a CaL plant to capture CO_2 from fossil fuels utilization, and (iv) the integration of both PV and CaL plants. A detailed flowsheet of the modelling of the system is shown in Fig. 3. The alumina production plant comprehends the main stages of Bayer process. Accordingly, the PV installation generates electricity to be used in digestion and evaporation stages of alumina production, as well as to pre-heat the aluminium hydroxide before its calcination in S200 and S400 scenarios. CaL configuration receives the flue gases from aluminium hydroxide calciner at the carbonation unit, and subsequently calcines the produced $CaCO_3$ in an oxy-fuel combustion. When both PV and CaL are implemented, solar-based electricity is also used in an air separation unit to produce oxygen for the oxy-fuel combustion.

Table 1
Proposed scenarios of the study.

Case Study	Electrification Temperature (°C)	Solar Photovoltaic System	Calcium-looping Plant
S100	100	–	–
S100-PV	100	✓	–
S100-CaL	100	–	✓
S100-PV-CaL	100	✓	✓
S200	200	–	–
S200-PV	200	✓	–
S200-CaL	200	–	✓
S200-PV-CaL	200	✓	✓
S400	400	–	–
S400-PV	400	✓	–
S400-CaL	400	–	✓
S4-PV-CaL	400	✓	✓

2.1. Simulation and optimization of alumina production

The simulation of a plant processing 1.5 million tonnes of bauxite per year was carried out incorporating the chemical reactions and energy balances across the diverse stages of the process to produce smelter grade alumina. The bauxite used in the study is characterized as gibbsite with a composition of 63.85%wt $Al(OH)_3$, 24.38%wt Fe_2O_3, 5.29%wt SiO_2, 3.84 % TiO_2 and 2.64%wt CaO [34].

The first stage of the process is the milling of bauxite to adequate its particle size for industrial processing. Afterwards, digestion of bauxite in NaOH solution occurs at 140 °C and 3 bar. CaO is also added to remove silica and avoid its dissolution into the liquor. The primary reaction that takes place in the digestors is shown in Reaction **(1)** [35].

$$Al(OH)_3\,(s) + NaOH\,(aq) \rightarrow Al(OH)_4^-\,(aq) + Na^+\,(aq)\ \Delta H_r^0 = 26.4\ kJ/mol\ Al(OH)_3 \quad (1)$$

Subsequently, a filtration stage is needed to separate solid and liquid phases. Solid phase, termed as bauxite residue, is composed by undissolved iron and titanium oxides, as well as calcium-silicate oxides. Bauxite residue is removed from the liquid and disposed in landfills after treatment [36], but bauxite residue management is out of scope in this study. Otherwise, the remaining liquid containing aluminium ions is sent to precipitator tanks, where the reverse reaction, shown in Reaction **(2)**, occurs at 70 °C to precipitate pure aluminium hydroxide.

$$Al(OH)_4^-\,(aq) + Na^+\,(aq) \rightarrow Al(OH)_3\,(s) + NaOH\,(aq) \quad (2)$$

After washing the solid, aluminium hydroxide is calcined at 1,100 °C in a natural gas-fired furnace with 5 % stoichiometric excess of air. The main chemical reactions that happen in the calciner are shown in Reaction **(3)** and Reaction **(4)**. Combustion heat of Reaction **(4)** elevates the temperature of $Al(OH)_3$ and provides the necessary thermal energy for Reaction **(3)** to occur completely.

$$CH_4\,(g) + 2O_2\,(g) \rightarrow 2H_2O\,(g) + CO_2\,(g)\ \Delta H_r^0 = -802.0\ MJ/mol\ CH_4 \quad (3)$$

$$2Al(OH)_3\,(s) \rightarrow Al_2O_3\,(s) + 3H_2O\,(g)\ \Delta H_r^0 = 185.2\ kJ/mol\ Al(OH)_3\ [37] \quad (4)$$

In case studies S100, solid aluminium hydroxides enter directly the calciner from the precipitator tanks at 70 °C, whereas in S200 and S400 case studies, solids are pre-heated through resistive electric heating up

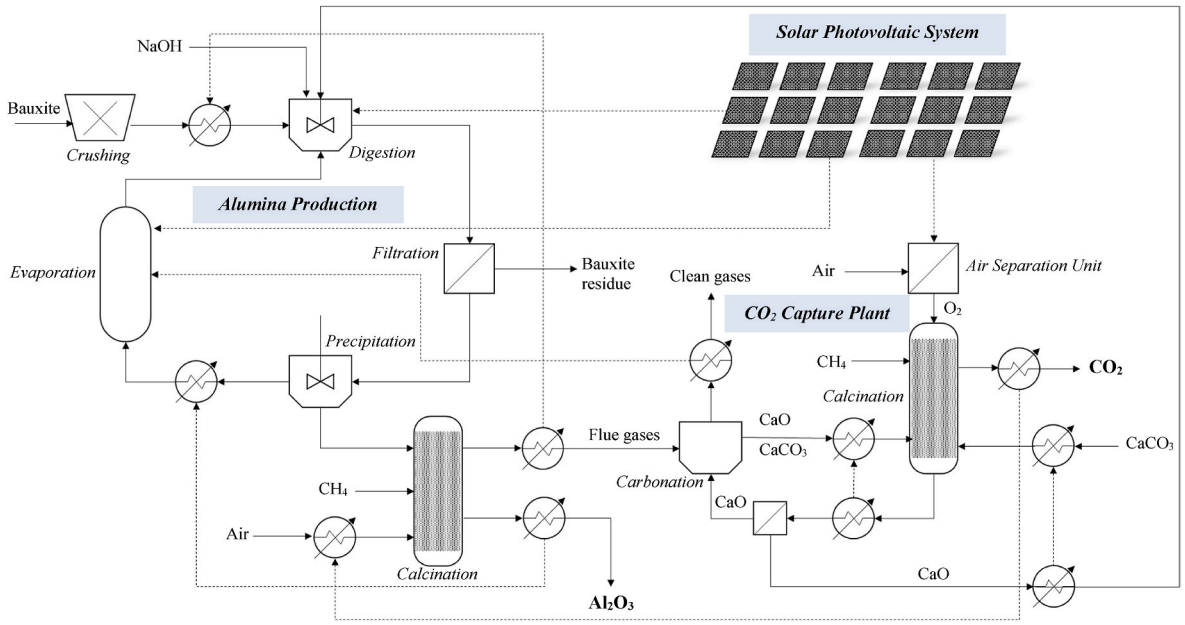

Fig. 3. Process flow diagram of the complete system.

to 200 and 400 °C respectively, decreasing the need of natural gas at the calciner. The remaining caustic liquor after precipitation is sent to an evaporator at 100 °C to re-concentrate NaOH and reuse it in the digestion stage. The complete list of technical assumptions and conditions considered are detailed in Table 2.

2.2. Solar photovoltaic system

After the simulation and optimization of the alumina production plant, a photovoltaic plant was dimensioned to obtain the electricity demand of the process in each case. The essential parameters for this dimensioning include the specifications of the solar panels, the total annual electrical energy output projected from these panels and the peak solar hour applicable to the location where the photovoltaic installation is sited.

Table 2
Technical assumptions and operating conditions considered in alumina refinery model.

Unit Process	Parameter	Value
Crushing	Initial particle size	D50 = 50 mm; σ = 1 mm
	Required particle size	<250 μm
	Bond Work Index	11 kWh/tonne
	Mechanical Efficiency	0.85
Digestion	Temperature	140 °C
	Pressure	3 bar
	Reaction (1) extent	97 % [55]
	NaOH input	50 kg/tonne Al_2O_3 [56]
	CaO input	18 kg/tonne Al_2O_3 [56]
Filtration	Solid removal	100 %
	Liquid/Solid ratio	0.18
Precipitation	Temperature	70 °C
	Pressure	1 bar
	Reaction (2) extent	99 %
Evaporation	Temperature	100 °C
Calcination	Temperature	1100 °C
	Pressure	1 bar
	Air input	5 % stoichiometric excess
	Reaction (3) extent	100 %
	Reaction (4) extent	100 %
Heat Exchangers System	Minimal temperature interval	30 °C

The considered solar panels are standard panels for industrial application (Jinko Tiger Pro HC 144cel) of 550W maximum power with a voltage of 40.9V and an amperage of 13.45A. Another parameter related to solar panels is the efficiency of the panel, whose losses related to temperature, wiring, dirt, inverter, shading, coupling, transformer, and auxiliary losses are estimated at 17 %. Degradation of PV panels over time is included as constant, as elevated temperatures are the main responsible for that degradation [38]. Hence, an efficiency of 83 % is considered for each panel [39].

Another important factor to be considered in the sizing of the photovoltaic installation is the location of the installation, as, depending on the location, the monthly solar irradiation values will vary. Solar irradiation takes into account the angle of the sun's rays, their impact on the Earth, as well as the orientation of the panels, shadows, and the climate of the region. The location considered in the simulation is a region with an average Mediterranean climate, considering the several alumina plants located in the south of Europe. The number of peak sun hours (PSH) was estimated at 2400 h per year. PSH is the number of hours that solar irradiation reaches 1000W/m^2, and it was calculated on a monthly basis using solar irradiation data from PVGIS databases from the European Commission Joint Research Center [40]. The number of necessary solar panels and the land occupation for the PV system were calculated using **Equation (1)** and **Equation (2)** respectively.

$$N = \frac{E}{A \cdot V \cdot PSH \cdot \gamma} \tag{1}$$

in which N is the number of standard solar photovoltaic panels, E is the electricity demand of the plant in MWh per year, A is the amperage and V is the voltage of the selected panels, PSH is the number of peak sun hours per year and γ is the efficiency of the solar panel, set at 0.83.

$$L = 1.02 \cdot 10^{-3} \cdot E \tag{2}$$

in which L is the land occupation measured in hm^2. **Equation (2)** was developed by analysing the land occupation of real PV plants located in eastern Spain as function of their net electricity production [41].

The use of batteries to store energy during solar hours on a daily basis is included on the purchased PV panels. However, lithium-ion batteries to store surplus electricity during summer months are not considered, because of the high economic costs that could be incurred. The variation of electricity production of the PV system assumed per month was

calculated proportionally to correction factors [42] commonly used to estimate solar irradiation in PV installations. These correction factors vary depending on the latitude of the location and the inclination angle of the panels [43]. A latitude of 41° N was assumed and an inclination angle of 35° was selected as the optimal. Accordingly, the deviation of monthly electricity production estimated for the location of the plant is shown in Fig. 4 with respect to the electricity demand of the process. Required electricity in lesser production months is assumed to be purchased externally, whereas electricity surpluses are assumed to be sold at half the price of the purchase cost.

2.3. Calcium-looping configuration

Calcium looping was selected as the proposed technology to capture post-combustion CO_2, aiming for the integration of the additional power that CaL generates [44]. The use of CaO as necessary precursor, which is largely available and relatively cheap [45], was also decisive for the choice of this study. The modelling of a CaL plant and its integration into the alumina refinery was performed using Aspen Plus V12.1 software [46]. The layout of the plant is shown in Fig. 3. The basis of the integration include the energy optimization of the processes and the use of purged CaO in the digestion stage of the alumina production process.

Combustion gases from aluminium hydroxide calcination of alumina refinery are sent to a carbonation unit to remove CO_2 and isolate it for its use or storage. At the carbonator, calcium oxide traps CO_2 at 650 °C according to Reaction **(5)**.

$$CaO\ (s) + CO_2\ (g) \rightarrow CaCO_3\ (s)\ \Delta H_r^0 = -178.0\ kJ/mol\ CaO \quad (5)$$

Sensible heat from CO_2-free gases is exploited in low-temperature processes of alumina production to decrease the electricity demand of the plant. Besides, the mixture of calcium carbonate and unreacted calcium oxide is heated up to 900 °C in an oxy-fuel calciner, where calcium carbonate decomposes following the reverse of Reaction **(5)**. A heat exchanger is proposed to preheat the air input of the alumina calciner using heat residues of CO_2 and vapour stream at 900 °C. Thus, thermal energy demand of the alumina plant decreases, which has a synergistic effect on the size of the CaL plant.

Finally, CaO is recycled back to the carbonation unit. However, to avoid the decay of sorption capacity of CaO, a purge of a small fraction of sorbent must be executed after the oxy-fuel combustion. This stream is used at the digestors of the alumina plant, assuming purged CaO is valid for the desilication of the ore prior to its digestion.

To develop the CaL model in Aspen Plus, a stoichiometric reactor was simulated as the carbonator, in which conversion of CaO was calculated using its number of carbonation/calcination cycles as a reference. Moreover, a calciner was also modelled as a free Gibbs energy minimization reactor. Average conversion of CaO sorbent at the carbonation unit was calculated according to **Equation (3)** [47].

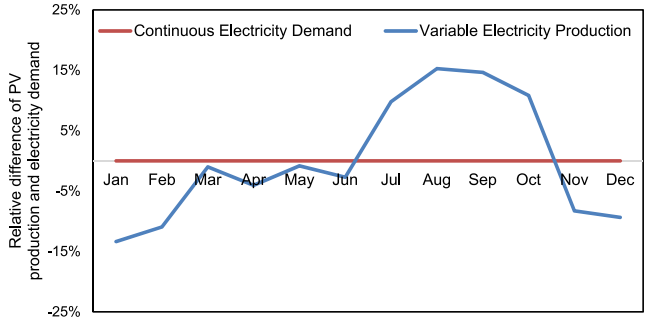

Fig. 4. Monthly deviation between constant electricity demand of alumina production and assumed electricity production of PV system.

$$X_{ave} = \sum_{Ncycles=1}^{Ncycles=\infty} r_N \cdot X_N \quad (3)$$

in which X_{ave} represents the average conversion of circulating CaO sorbent and N_{cycles} is the number of cycles of each CaO particle. X_N represents the conversion of one single particle of CaO and r_N is the percentage of CaO particles that have gone through N_{cycles} number of cycles.

The conversion of one single particle of circulating CaO can be calculated as presented in **Equation (4)** [32].

$$X_N = \frac{1}{\frac{1}{1-X_r} + k \cdot N_{cycles}} + X_r \quad (4)$$

in which the parameter k is a sorption decay constant dependent on the type of sorbent and X_r is the residual activity of the sorbent. For this study, values of $k = 0.52$ and $X_r = 0.075$ were assumed [32].

The percentage of CaO particles that have suffered N_{cycles} number of carbonation-calcination cycles, r_N, can be estimated as shown in **Equation (5)** [47].

$$r_N = \frac{\frac{F_{CaCO3}}{F_{CaO}}}{\left(1 + \frac{F_{CaCO3}}{F_{CaO}}\right)^{N_{cycles}}} \quad (5)$$

in which F_{CaCO3} and F_{CaO} are the molar flowrates of fresh calcium carbonate that enters the calciner and the recycled calcium oxide that enters the carbonator respectively.

Configurations with low purges of sorbent and high CaO/CO_2 ratios on the carbonation unit are preferred to minimize the energy consumption and optimize economic costs, as long as CO_2 capture is efficient enough [33]. To calculate molar flowrates of fresh limestone and recycled CaO, two parameters were considered. First, the purge ratio of CaO sorbent was fixed at 2.5 %, i.e. 97.5 % of sorbent was recycled back to the carbonator. Moreover, molar ratio of CaO/CO_2 entering the carbonation unit varied around 4.5–5.5 depending on the scenario, ensuring the capture of at least 96 % of initial CO_2 emitted.

Main technical assumptions and operating conditions of the CaL plant modelled are listed on Table 3.

2.4. Economic assessment

Economic performance of the different models were evaluated using the Net Present Value (NPV) calculation, considering an existing alumina production plant. Payback time (PB) was also estimated for scenarios in which capital expenditures on PV and CaL plants were necessary. NPV and PB were calculated as shown in Equation 6 [48] and Equation 7 [48] respectively.

$$NPV = \sum_{t=1}^{n} \frac{V_T}{(1+i)^t} - I_0 \quad (6)$$

Table 3
Technical assumptions and operating conditions considered for CaL model.

Unit Process	Parameter	Value
Carbonation	Temperature	650 °C
	CaO/CO_2 ratio	4.5–5.5
	CaO purge ratio	2.5 %
	Reaction (5) extent	Equation 4
Calcination	Temperature	900 °C
	Oxygen input	Stoichiometric
	Calcination extent	Free Gibbs energy minimization
Air Separation Unit	Energy Consumption	813.6 MJ/t O_2 [57]
Heat Exchangers System	Minimal temperature interval	30 °C

$$PB = \frac{I_0}{V_T - V_0} \quad (7)$$

where V_T represents the cash flows after taxes of each period t, I_0 represents the initial capital investments, n is the total number of periods considered and i represents the discount rate. To calculate payback time of the investment in each case, net profits of PV and CaL integrations are considered. Hence, V_0 represents the cash flow after taxes of each base case (S100, S200 and S400).

The period of time considered for the calculation of NPV was set at 25 years, comprehending the cash flows periods of 1 year each. The discount rate was set at 0.08, considering the weighted average cost of capital of aluminium companies [22]. The complete list of economic considerations assumed to calculate the annual cash flows are summarized on Table 4. Current CO_2 emission taxes of 85€ per tonne were considered [49], as well as a grid electricity cost of 0.076 €/kWh [50]. Nevertheless, sensitivity analysis were performed to assess the consequences of market fluctuations of these parameters.

Purchase equipment costs of the PV system were calculated assuming a cost of 170€ per standard solar photovoltaic panel [51]. Purchase equipment costs of CaL plant are primarily made up of carbonation, oxy-fuel calcination and air separation units. Purchase equipment costs of these units were calculated as a function of their thermal energy output, thermal energy input and mass flow of oxygen produced respectively, as shown in Table 5. A factor of 3.60 was added to CaL units to estimate total direct costs of the CaL plant (auxiliary equipment, installation, electrical systems, piping, service facilities, building …) [52]. Another factor of 1.26 and 1.44 was used to estimate indirect costs (construction expenses, legal expenses, contingencies …) related to PV and CaL systems respectively [52]. The summary of the methodology followed to estimate capital expenditures of both PV and CaL plants is shown in Table 5. Equations for the estimation of CaL plant were retrieved from Horizon 2020 CEMCAP project [53] and a 1.37 factor was added, based on the Chemical Engineering Plant Cost Index, to update costs to 2024 prices.

3. Results and discussion

3.1. Energy performance

Results of alumina refinery simulations indicate that 0.40 tonnes of smelter grade alumina are produced per tonne of processed bauxite, whereas approximately 0.51 tonnes of bauxite residue are discarded per tonne of bauxite. Hence, 1.26 tonnes of bauxite residue are produced per tonne of alumina. This results are merely a consequence of the composition of bauxite assumed. Alumina refinement is estimated to produce around 1–1.5 tonnes of bauxite residue per tonne of alumina produced, depending on the composition and quality of bauxite [54], which agrees with the results of this model. Effects of bauxite composition are also observable on energy requirement levels. Generally, energy demand of alumina production process is in the range of 8500–11800 MJ per tonne of alumina produced [6]. In this study, energy consumption of single alumina plant varies mildly around 10714–10765 MJ per tonne of alumina, depending on the electrification scenario, which validates the model and the initial assumptions assumed.

Global energy demands of the different cases of this study are listed in Table 6. Results indicate that direct electrification has a slight impact on global energy consumption. Electrifying first stage of hydroxide calcination up to 400 °C reduces only 0.5 % the energy use of the base alumina plant, from 2.990 MWh to 2.976 MWh per tonne of alumina. However, this small change can result into a good mitigation strategy for CO_2 emissions, since gas-based thermal energy consumption decreases over 15 %, from 2.546 MWh_{th} to 2.159 MWh_{th} per tonne of alumina. Estimated CO_2 direct and indirect emissions are shown in Fig. 5 for each of the scenarios analysed. Indirect emissions from grid electricity generation were calculated using an emission factor of 275 kg of CO_2 eq. per MWh. As shown in Fig. 5, electrification at 400 °C can induce a 15.2 % reduction of direct CO_2 emissions, from 504.2 to 427.6 kg $CO_{2\text{-eq}}$ per tonne of alumina. Additionally, if renewable electricity generation is implemented, CO_2 equivalent emissions can be reduced nearly 30 %, from 626.4 to 437.0 kg of $CO_{2\text{-eq}}$ per tonne of alumina produced. Therefore, it can be of interest to propose the electrification and production of renewable electricity within alumina industry.

In regards to the integration of a CaL plant into an alumina refinery, results show an energy penalty of 6–7% for capturing 97 % of CO_2 emissions, increasing the energy demand from 2.976 to 2.990 MWh to 3.146–3.172 MWh per tonne of alumina produced. The existence of low-temperature processes during alumina production, like ore digestion

Table 4
Conditions considered in the economic assessment.

	Value	Reference
Capital expenses		
Planned lifetime, *n* (years)	25	
Discount rate, *i*	0.08	
Effective tax rate (%)	35.00	
Material Inputs		
Bauxite cost (€/tonne)	20	[36]
CaO cost (€/tonne)	60	
NaOH cost (€/tonne)	345	
$CaCO_3$ cost (€/tonne)	20	[58]
Water cost (€/tonne)	0.10	
Energy Inputs		
Natural Gas cost (€/kWh)	0.041	[59]
Grid electricity cost (€/kWh)	0.076	[50]
Outputs		
Bauxite residue disposal cost (€/tonne)	9.13	[36]
CO_2 emission taxes (€/tonne)	85.00	[49]
Wastewater spill cost (€/tonne)	0.20	
CO_2 storage cost (€/tonne)	7.00	[60]
Alumina revenue (€/tonne)	365	[36]

Table 5
Estimation of capital expenditures of PV and CaL systems.

	Equation	Ref.
PV System		
Purchased Equipment Cost (PEC) (M€)	$1.70{\cdot}10^{-4}$ *N (number of panels)*	[51]
Total Capital Cost (M€)	1.26·*PEC*	[52]
CaL System		
Air Sep Unit Purchased Cost (ASU) (M€)	$1.37{\cdot}8.817{\cdot}(O_2$ *mass flow* [kg/s]$)^{0.6}$	[53]
Carbonator Purchased Cost (CPC_1) (M€)	*1.37·(Thermal Output* [MW_{th}]·*0.217 + 3.83)*	[53]
Calciner Purchased Cost (CPC_2) (M€)	$1.37{\cdot}0.193{\cdot}$(*Thermal Input* [MW_{th}]$)^{0.65}$	[53]
Total Capital Cost (M€)	1.44·*ASU* + 4.04·*(CPC_1 + CPC_2)*	[52]

Table 6
Electricity (MWh_e) and natural gas (MWh_{th}) consumption in each scenario per tonne of alumina produced.

Plant	Energy	S100		S200		S400	
		–	CaL	–	CaL	–	CaL
Alumina Refinery	Thermal Energy	2.546	1.775	2.393	1.664	2.159	1.502
	PV/Grid Electricity	0.444	0.712	0.591	0.833	0.817	1.025
CaL Plant	Thermal Energy	–	0.615	–	0.597	–	0.563
	PV/Grid Electricity	–	0.070	–	0.068	–	0.064
Total Energy Consumption (MWh/tonne Al_2O_3)		2.990	3.172	2.985	3.162	2.976	3.154

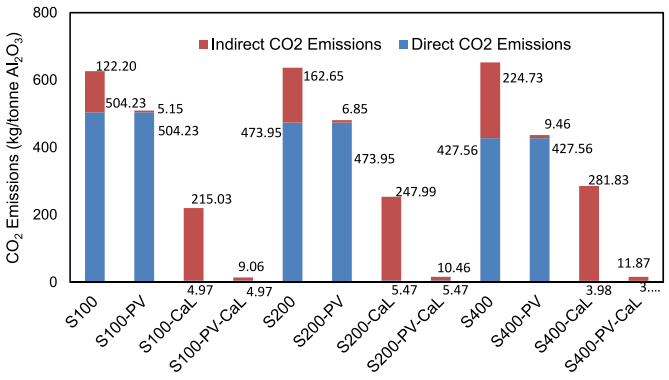

Fig. 5. Estimated CO_2 emissions from thermal energy and electricity consumption for each case study of the analysis.

and evaporation, eases the energy recovery of the oxy-fuel combustion unit, showing a low energy penalty of 0.364–0.401 MWh per tonne of CO_2 avoided. As shown in Table 6, the integration of a CaL plant allows for a displacement in natural gas consumption, decreasing drastically the thermal energy demand of alumina production at high temperature levels. Overall fossil consumption remains similar, as heat surpluses are exploited at the alumina calciner. Hence, CaL configuration performs as a promising solution if mid-temperature electrification is possible and renewable electricity is available. Fig. 5 shows the results of nearly zero CO_2 emissions from combined PV and CaL plants, whereas single integration of CaL plant shows the energy displacement, achieving the capture of fossil fuel emissions but increasing the emissions from electricity generation.

3.2. Economic performance

NPV calculations were performed considering a grid electricity cost of 0.076 €/kWh$_e$, a natural gas cost of 0.041 €/kWh$_{th}$ and a carbon emission tax of 85 € per tonne of CO_2 emitted. According to these conditions, NPV, annual cash flows after taxes, capital expenditures and payback time of each investment are shown in Table 7. Additionally, NPV and annual cash flow after taxes are also represented in Figs. 6 and 7 respectively. As shown in Table 7, base cases of an alumina production plant of 1.5 million tonnes of bauxite per year are highly profitable, which may hinder the implementation of new technologies. However, the addition of a PV system appears to be an effective strategy, especially if high electrification levels are implemented. With medium investments (68.5–125.9 M€), NPV increases around 30–60 % with respect to the base cases, with a payback time of the investment of 4.5 years. The main disadvantage in this case is the land occupation for the integration of the

Table 7
NPV, annual cash flow, capital expenditures (CAPEX) and payback time of each case study.

Case Study	NPV (M€)	Annual Cash Flow (M€)	CAPEX (M€)	Payback time (years)
S100	299.06	28.02	–	–
S100-PV	393.15	43.25	68.48	4.50
S100-CaL	213.09	34.96	160.13	23.05
S100-PV-CaL	378.64	61.76	280.64	8.32
S200	285.61	26.76	–	–
S200-PV	410.83	43.41	91.15	5.47
S200-CaL	198.66	33.24	156.11	24.09
S200-PV-CaL	389.57	64.14	295.09	7.89
S400	264.83	24.81	–	–
S400-PV	437.85	52.82	125.94	4.49
S400-CaL	199.11	32.71	150.08	18.99
S4-PV-CaL	416.09	67.83	308.02	7.16

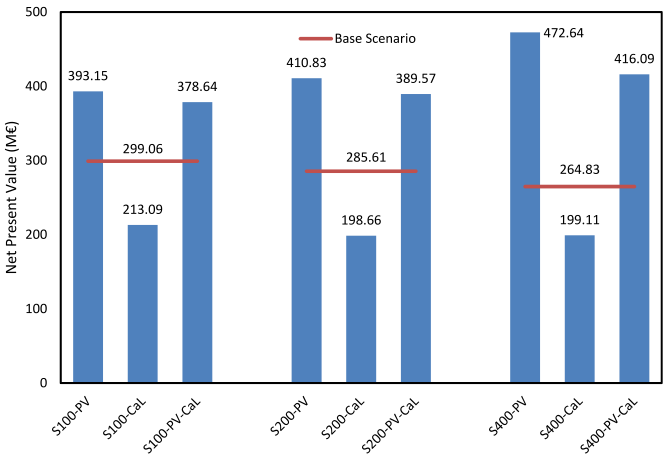

Fig. 6. Net Present Value estimation for each case study.

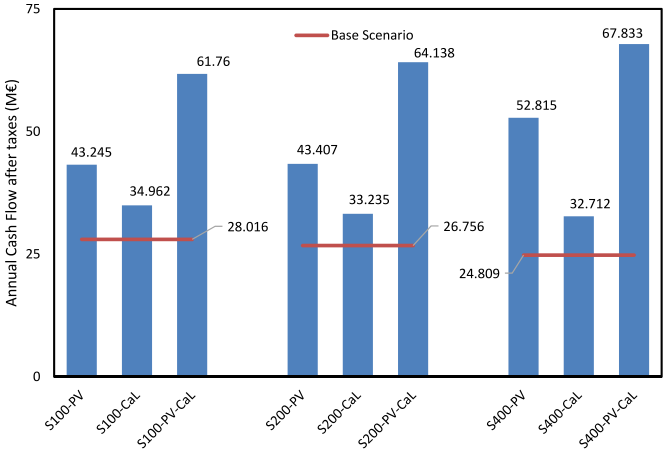

Fig. 7. Annual cash flow after taxes estimated for each case study.

PV system. For an alumina plant that treats 1.5 million tonnes of bauxite per year, producing approximately 0.6 million tonnes of alumina, land occupation is estimated at 270 hm^2 for 100 °C electrification temperature and 500 hm^2 when electrification temperature is 400 °C.

The integration of a CaL system is also challenging. Although the reduction of CO_2 emissions entails an enhancement of cash flows in all cases, the high capital expenses estimated for CaL technology (150–160 M€) can be a drawback for its implementation. Estimated NPV of CaL integration is 24–30 % reduced, whereas the calculated payback time increases around 19–24 years. The integration of both PV and CaL plants appears to be a safe strategy, since the reductions on electricity costs and carbon taxes make cash flows double its profits. However, the capital expenses of integrating both plants stand around 280–308 M€, with a payback time of 7–8 years. Cost reductions of CaL capital expenditures and/or more reliable cost estimations shall be crucial for CaL feasibility.

Regarding the electrification levels, increasing the target temperature of direct resistive heating benefits the economic performance of scenarios in which PV system is implemented. NPV of 400 °C electrification increases 9–11 % with respect to 100 °C electrification level. However, scenarios in which grid electricity purchase is considered, NPV falls 7–11 %. To detach the effects of electricity costs or carbon emission rights in economic evaluations, sensitivity analysis were carried out with three different grid electricity purchase prices (0.03, 0.09 and 0.15 €/kWh) and three different levels of carbon emissions taxes (50, 100 and 150 €/tonne of CO_2). Results of this sensitivity analysis are shown in Fig. 8.

Fig. 8 shows that, for cheap electricity prices, base scenarios result in

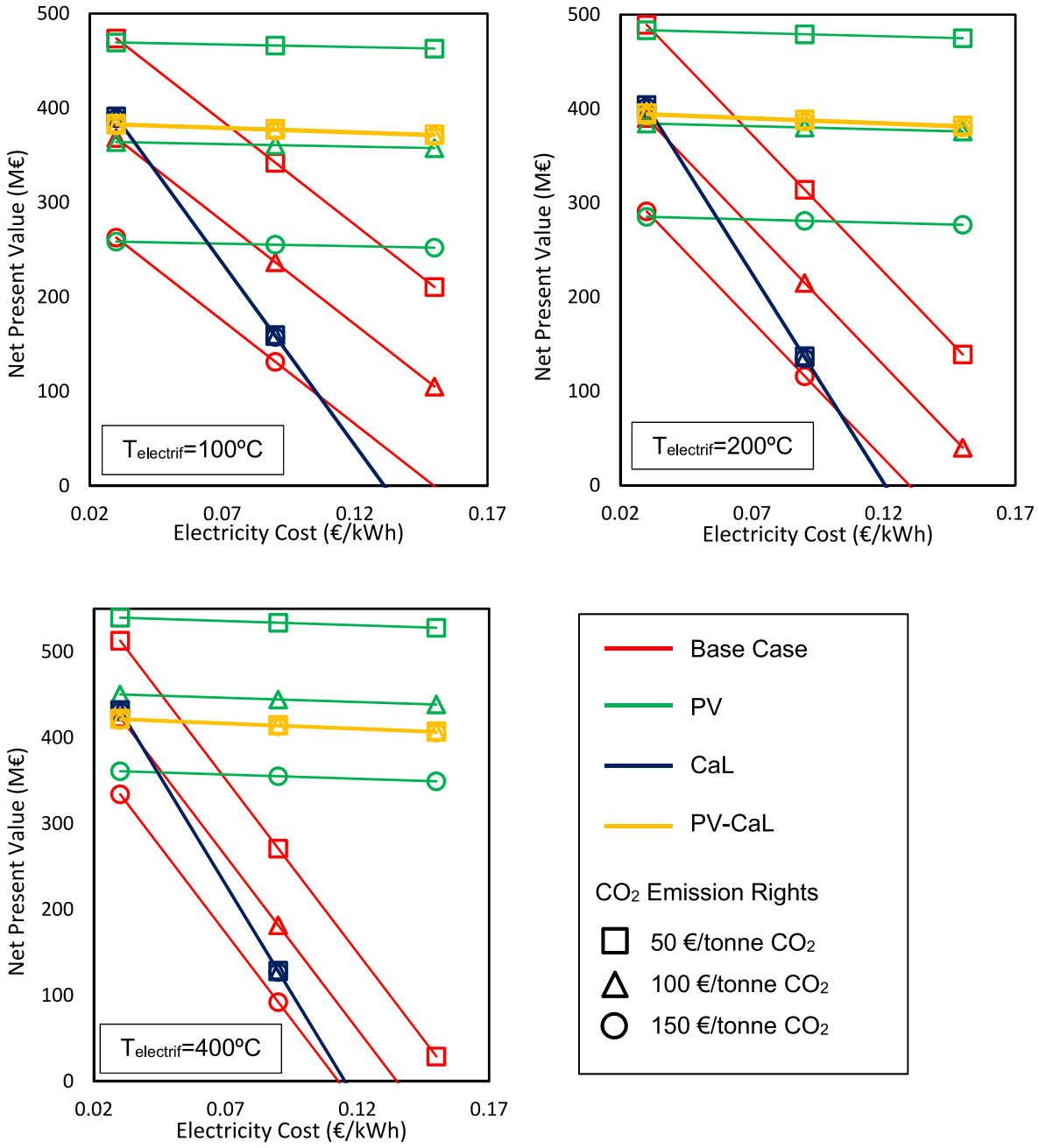

Fig. 8. Sensitivity analysis: variation of NPVs as a function of grid electricity prices and CO_2 emission taxes.

a better economic performance. However, as grid electricity cost increases, NPVs of base cases suffer a strong decay, whereas PV implemented systems remain practically unaffected by electricity costs fluctuations. Implementation of PV system shows better economic performance as long as grid electricity cost remain over 0.032 €/kWh. This gives an idea of the significance that developing own electricity generation systems can have on alumina industry.

Similar thing happens with CO_2 emission rights. For low carbon taxes, the investment of a CaL plant is not profitable, as base and PV cases show a greater economic performance. However, as carbon emission taxes varies in the range of 95–125 €/tonne, CaL integration becomes an interesting strategy in the search for better economic profit. The integration of both PV and CaL systems in alumina industry shows how NPVs remain nearly unchanged with variations of electricity costs and carbon taxes, with values of 380–410 M€ depending on the electrification level. This stands out as the most valuable scenario, as long as the carbon emission rights remain above 95 €/tonne.

Differences among electrification temperature levels show the interest of direct electrification of alumina industry. Economic performance of 400 °C electrification is upgraded in most of the cases, because of the reductions on energy consumption and the lesser CO_2 emissions. However, implementation of renewable electricity generation systems is recommended if direct electrification is pursued. Otherwise, dependence on electricity market becomes very remarkable, which could lead to worse economic results.

4. Conclusions

The production of alumina stands as an essential sector within raw material industries. Hence, mitigation of carbon emissions and environmental impacts of alumina production constitutes primary industrial concerns. In this context, while various studies have proposed

alternatives to reduce bauxite residue production or to valorise the residues, there is a lack of investigations that rigorously assess the thermal energy demands of Bayer process and potential strategies for decarbonisation.

Accordingly, in this work two coupled strategies were assessed to achieve carbon neutrality of alumina industry: electrification through direct resistive heating and CO_2 capture via calcium-looping technology. The modelling of an alumina refinery and the integration of both strategies showed that direct electrification of low and mid-temperature processes has a very slight effect on energy consumption, decreasing the energy demand a 0.5 %, from 2.990 MWh to 2.976 MWh per tonne of alumina. However, direct electrification can effectively reduce 15 % CO_2 direct emissions, estimated at 504.2 kg of CO_2 per tonne of alumina and 427.6 kg if electrification at 400 °C is implemented.

Inversely, calcium looping implementation can achieve the capture of 97 % of CO_2 emissions with an energy penalty below 7 % of energy consumption of an alumina production plant. In this case, the specific primary energy consumption per tonne of CO_2 avoided amounted to 0.364–0.401 MWh, standing out as a promising alternative. Through direct electrification at low temperatures, energy penalty of CO_2 capture can become nearly 100 % electrical, not increasing the fossil fuel depletion.

Economic performance of implementing a solar photovoltaic installation to self-supply electricity and a calcium-looping plant were also evaluated to study the feasibility of the proposals. The calculation of the net present values of the different case studies showed the good profitability of current alumina production, but also a big room for improvement with the installation of in-site electricity generation via solar photovoltaic panels. Net present value of solar photovoltaic implementation can increase 30–60 % depending on the electrification level, with a low payback time of 4.5 years. However, the implementation of a calcium-looping plant is hindered by the high capital expenses, showing a payback time of approximately 19–24 years.

The results of a sensitivity analysis concluded that in-site renewable electricity generation is a suitable solution, provided that grid electricity costs remain over 0.032 €/kWh. Carbon emission taxes can also play a crucial role in alumina industry. Carbon rights around 95–120 €/tonne of CO_2 can make feasible the investment on a CO_2 capture plant, leading to a process neutral in carbon emissions and economically profitable.

Despite potential deviations of this study from real industrial plants and constraints regarding estimation of capital expenses, findings of this work bring significant evidence about the options for environmentally friendly strategies in alumina industry, with limited negative consequences on the economic performance. Direct electrification and CO_2 capture after combustion can lead the way towards a complete sustainable alumina production, along with alternatives to avoid bauxite residue production.

CRediT authorship contribution statement

Javier Sáez-Guinoa: Writing – review & editing, Writing – original draft, Visualization, Software, Methodology, Investigation, Formal analysis, Conceptualization. **Inés Senante:** Resources, Investigation. **Eva Llera-Sastresa:** Writing – review & editing, Supervision, Conceptualization. **Luis M. Romeo:** Writing – review & editing, Supervision, Project administration, Funding acquisition, Conceptualization.

Declaration of competing interest

The authors declare that they have no known competing financial interests or personal relationships that could have appeared to influence the work reported in this paper.

Data availability

Data will be made available on request.

Acknowledgements

This work has been carried out in the frame of the AlSiCal project, funded by the European Union's Horizon 2020 research and innovation programme under grant agreement N. 820911. The work described in this paper is also partially supported by the Government of Aragon (Research Group DGA T46_23R: Energía y CO_2). Aspen Technology Inc. is also acknowledged for the use of the software.

References

[1] International Energy Agency, Energy technology perspectives 2020, Energy Technol. Perspect. 2020 (2020), https://doi.org/10.1787/ab43a9a5-en.
[2] International Energy Agency, Energy technology perspectives 2023, Energy Technol. Perspect. 2023 (2023), https://doi.org/10.1787/7C6B23DB-EN.
[3] B. Cushman-Roisin, B.T. Cremonini, Materials, data, stat. Useful numbers, Environ. Sustain. (2021) 1–16, https://doi.org/10.1016/B978-0-12-822958-3.00012-1.
[4] S.H. Farjana, N. Huda, M.A.P. Mahmud, Impacts of aluminum production: a cradle to gate investigation using life-cycle assessment, Sci. Total Environ. 663 (2019) 958–970, https://doi.org/10.1016/j.scitotenv.2019.01.400.
[5] Metallurgical Alumina Refining Energy Intensity - International Aluminium Institute, (n.d.). https://international-aluminium.org/statistics/metallurgical-alumina-refining-energy-intensity/(accessed March 12, 2024).
[6] J. Sáez-Guinoa, E. García-Franco, E. Llera-Sastresa, L.M. Romeo, The effects of energy consumption of alumina production in the environmental impacts using life cycle assessment, Int. J. Life Cycle Assess. 29 (2024) 380–393, https://doi.org/10.1007/S11367-023-02257-8.
[7] Primary Aluminium Smelting Energy Intensity - International Aluminium Institute, (n.d.). https://international-aluminium.org/statistics/primary-aluminium-smelting-energy-intensity/(accessed March 12, 2024).
[8] T.E. Norgate, S. Jahanshahi, W.J. Rankin, Assessing the environmental impact of metal production processes, J. Clean. Prod. 15 (2007) 838–848, https://doi.org/10.1016/j.jclepro.2006.06.018.
[9] S. Sgouridis, M. Ali, A. Sleptchenko, A. Bouabid, G. Ospina, Aluminum smelters in the energy transition: optimal configuration and operation for renewable energy integration in high insolation regions, Renew. Energy 180 (2021) 937–953, https://doi.org/10.1016/J.RENENE.2021.08.080.
[10] A. Shen, J. Zhang, Technologies for CO2 emission reduction and low-carbon development in primary aluminum industry in China: a review, Renew. Sustain. Energy Rev. 189 (2024) 113965, https://doi.org/10.1016/J.RSER.2023.113965.
[11] J. Wang, Q. Zhao, P. Ning, S. Wen, Greenhouse gas contribution and emission reduction potential prediction of China's aluminum industry, Energy 290 (2024) 130183, https://doi.org/10.1016/J.ENERGY.2023.130183.
[12] Y. Ma, A. Preveniou, A. Kladis, J.B. Pettersen, Circular economy and life cycle assessment of alumina production: simulation-based comparison of Pedersen and Bayer processes, J. Clean. Prod. 366 (2022) 132807, https://doi.org/10.1016/J.JCLEPRO.2022.132807.
[13] G. tao Zhou, Y. lin Wang, Y. guan Zhang, T. gui Qi, Q. sheng Zhou, G. hua Liu, Z. hong Peng, X. bin Li, A clean two-stage Bayer process for achieving near-zero waste discharge from high-iron gibbsitic bauxite, J. Clean. Prod. 405 (2023) 136991, https://doi.org/10.1016/J.JCLEPRO.2023.136991.
[14] Y. Wang, X. Li, Q. Zhou, B. Wang, T. Qi, G. Liu, Z. Peng, J. Pi, Z. Zhao, M. Wang, Reduction of red mud discharge by reductive bayer digestion: a comparative study and industrial validation, JOM 72 (2020) 270–277, https://doi.org/10.1007/S11837-019-03874-1/FIGURES/6.
[15] G. Lu, T. Zhang, F. Guo, X. Zhang, Y. Wang, W. Zhang, L. Wang, Z. Zhang, Clean and efficient utilization of low-grade high-iron sedimentary bauxite via calcification-carbonation method, Hydrometallurgy 187 (2019) 195–202, https://doi.org/10.1016/J.HYDROMET.2019.04.027.
[16] O. Agboola, D.E. Babatunde, O.S. Isaac Fayomi, E.R. Sadiku, P. Popoola, L. Moropeng, A. Yahaya, O.A. Mamudu, A review on the impact of mining operation: monitoring, assessment and management, Results Eng 8 (2020) 100181, https://doi.org/10.1016/J.RINENG.2020.100181.
[17] G.T. Zhou, Y.L. Wang, T.G. Qi, Q.S. Zhou, G.H. Liu, Z.H. Peng, X. Bin Li, Toward sustainable green alumina production: a critical review on process discharge reduction from gibbsitic bauxite and large-scale applications of red mud, J. Environ. Chem. Eng. 11 (2023) 109433, https://doi.org/10.1016/J.JECE.2023.109433.
[18] R. Lundmark, E. Wetterlund, E. Olofsson, On the green transformation of the iron and steel industry: market and competition aspects of hydrogen and biomass options, Biomass Bioenergy 182 (2024) 107100, https://doi.org/10.1016/J.BIOMBIOE.2024.107100.
[19] D.S. Mallapragada, Y. Dvorkin, M.A. Modestino, D.V. Esposito, W.A. Smith, B. M. Hodge, M.P. Harold, V.M. Donnelly, A. Nuz, C. Bloomquist, K. Baker, L. C. Grabow, Y. Yan, N.N. Rajput, R.L. Hartman, E.J. Biddinger, E.S. Aydil, A. D. Taylor, Decarbonization of the chemical industry through electrification: barriers and opportunities, Joule 7 (2023) 23–41, https://doi.org/10.1016/J.JOULE.2022.12.008.
[20] M. Simoni, M.D. Wilkes, S. Brown, J.L. Provis, H. Kinoshita, T. Hanein, Decarbonising the lime industry: state-of-the-art, Renew. Sustain. Energy Rev. 168 (2022) 112765, https://doi.org/10.1016/J.RSER.2022.112765.
[21] South 32, Annual Report 2018 - Environment, 2018.
[22] Norsk Hydro ASA, Integrated Annual Report 2023, 2024.

[23] Rio Tinto and Sumitomo to build Gladstone hydrogen pilot plant to trial lower-carbon alumina refining, (n.d.). https://www.riotinto.com/en/news/releases/2023/rio-tinto-and-sumitomo-to-build-gladstone-hydrogen-pilot-plant-to-trial-lower-carbon-alumina-refining (accessed March 13, 2024).
[24] Alcoa – Refinery of the Future, (n.d.). https://www.alcoa.com/global/en/what-we-do/alumina/refinery-of-the-future (accessed March 13, 2024).
[25] Alcoa to investigate low emissions alumina - Australian Renewable Energy Agency (ARENA), (n.d.). https://arena.gov.au/news/alcoa-to-investigate-low-emissions-alumina/(accessed March 13, 2024).
[26] European Commission, Innovation Fund - Driving Clean Innovative Technologies towards the Market, 2021.
[27] F. Hossain, M.J. Hasan, M.Z. Sarkar, M.R. Karim, A.A. Bhuiyan, Prediction of carbon capture and sequestration (CCS) technology in a 125 MW tangentially coal-fired subcritical thermal power plant for retrofitting in Bangladesh, Results Eng 18 (2023) 101159, https://doi.org/10.1016/J.RINENG.2023.101159.
[28] J. Perpiñán, B. Peña, M. Bailera, V. Eveloy, P. Kannan, A. Raj, P. Lisbona, L. M. Romeo, Integration of carbon capture technologies in blast furnace based steel making: a comprehensive and systematic review, Fuel 336 (2023) 127074, https://doi.org/10.1016/J.FUEL.2022.127074.
[29] A. Peppas, C. Politi, S. Kottaridis, M. Taxiarchou, LCA analysis decarbonisation potential of aluminium primary production by applying hydrogen and CCUS technologies, Hydrogen 4 (2023) 338–356, https://doi.org/10.3390/hydrogen4020024.
[30] J. Sáez-Guinoa, I. Senante, S. Pascual, E. Llera-Sastresa, L.M. Romeo, [Under Review] Eco-efficiency assessment of carbon capture and hydrogen transition as decarbonisation strategies in alumina production, J. Clean. Prod. (2024).
[31] L.M. Romeo, D. Catalina, P. Lisbona, Y. Lara, A. Martínez, Reduction of greenhouse gas emissions by integration of cement plants, power plants, and CO2 capture systems, Greenh, Gases Sci. Technol. 1 (2011) 72–82, https://doi.org/10.1002/GHG3.5.
[32] G.S. Grasa, J.C. Abanades, CO2 capture capacity of CaO in long series of carbonation/calcination cycles, Ind. Eng. Chem. Res. 45 (2006) 8846–8851, https://doi.org/10.1021/ie0606946.
[33] L.M. Romeo, Y. Lara, P. Lisbona, J.M. Escosa, Optimizing make-up flow in a CO2 capture system using CaO, Chem. Eng. J. 147 (2009) 252–258, https://doi.org/10.1016/j.cej.2008.07.010.
[34] L.K. Hudson, C. Misra, A.J. Perrotta, K. Wefers, F.S. Williams, Aluminum oxide, in: Ullmann's Encycl, second ed., Ind. Chem., 2012, pp. 607–644, https://doi.org/10.1002/14356007.a01_557.
[35] J.A.M. Pereira, M. Schwaab, E. Dell'Oro, J.C. Pinto, J.L.F. Monteiro, C. A. Henriques, The kinetics of gibbsite dissolution in NaOH, Hydrometallurgy 96 (2009) 6–13, https://doi.org/10.1016/J.HYDROMET.2008.07.009.
[36] S.M.A. Qaidi, B.A. Tayeh, H.F. Isleem, A.R.G. de Azevedo, H.U. Ahmed, W. Emad, Sustainable utilization of red mud waste (bauxite residue) and slag for the production of geopolymer composites: a review, Case Stud. Constr. Mater. 16 (2022) e00994, https://doi.org/10.1016/J.CSCM.2022.E00994.
[37] D. Davis, F. Müller, W.L. Saw, A. Steinfeld, G.J. Nathan, Solar-driven alumina calcination for CO 2 mitigation and improved product quality, Green Chem. 19 (2017) 2992–3005, https://doi.org/10.1039/C7GC00585G.
[38] T. Rahman, A. Al Mansur, M.S. Hossain Lipu, M.S. Rahman, R.H. Ashique, M. A. Houran, R.M. Elavarasan, E. Hossain, Investigation of degradation of solar photovoltaics: a review of aging factors, impacts, and future directions toward sustainable energy management, Energies 2023 16 (2023) 3706, https://doi.org/10.3390/EN16093706. Page 3706 16.
[39] Satel, Planta Fotovoltaica "Campo De Belchite 2 (2020). http://coiiar.e-visado.net.
[40] B.E. Psiloglou, H.D. Kambezidis, D.G. Kaskaoutis, D. Karagiannis, J.M. Polo, Comparison between MRM simulations, CAMS and PVGIS databases with measured solar radiation components at the Methoni station, Greece, Renew. Energy 146 (2020) 1372–1391, https://doi.org/10.1016/J.RENENE.2019.07.064.
[41] Boletín Oficial de Aragón, Competitividad y Desarrollo Empresarial de Zaragoza, por el que se somete a información pública, la solicitud de autorización administrativa previa y de construcción, del proyecto Planta Solar Fotovoltaica, Ca, Spain, 2020. ANUNCIO del Servicio Provincial de Industria.
[42] J.M. Fernández Salgado, Guía completa de la energía solar térmica y termoeléctrica : (adaptada al Código Técnico de la Edificación y al nuevo RITE), A. Madrid Vicente, 2010. Madrid.
[43] R.K. Aggarwal, New correction factor for the estimation of solar radiation, J. Renew. Sustain. Energy 1 (2009), https://doi.org/10.1063/1.3192749.
[44] B. Duhoux, R.T. Symonds, R. Hughes, P. Mehrani, E.J. Anthony, A. Macchi, Simulation of a calcium looping CO2 capture process for pressurized fluidized bed combustion, Can. J. Chem. Eng. 98 (2020) 75–83, https://doi.org/10.1002/CJCE.23569.
[45] C. Ortiz, J.M. Valverde, R. Chacartegui, Energy consumption for CO2 capture by means of the calcium looping process: a comparative analysis using limestone, dolomite, and steel slag, Energy Technol. 4 (2016) 1317–1327, https://doi.org/10.1002/ENTE.201600390.
[46] Aspen Plus | Leading Process Simulation Software | AspenTech, (n.d.). https://www.aspentech.com/en/products/engineering/aspen-plus (accessed February 14, 2024).
[47] S. Pascual, P. Lisbona, M. Bailera, L.M. Romeo, Design and operational performance maps of calcium looping thermochemical energy storage for concentrating solar power plants, Energy 220 (2021) 119715, https://doi.org/10.1016/J.ENERGY.2020.119715.
[48] E.R. Yescombe, Macro-economic risks, in: Princ. Proj. Financ., Academic Press, 2014, pp. 257–294, https://doi.org/10.1016/B978-0-12-391058-5.00010-2.
[49] European Commission, Report from the Commission to the European Parliament and the Council on the Functioning of the European Carbon Market in 2022 Pursuant to Articles 10(5) and 21(2) of Directive 2003/87, EC, 2023.
[50] European Commission; Directorate-General for Energy unit A4 Market Observatory for Energy, Quarterly Report on European Electricity Markets, 2021.
[51] Potente placa solar 550W Jinko Tiger Pro, (n.d.) https://www.monsolar.com/placa-jinko-tiger-pro.html (accessed March 18, 2024).
[52] M.S. Peters, K.D. Timmerhaus, R.E. West, Plant Design and Economics for Chemical Engineers, fifth ed., 2003.
[53] R. Anantharaman, D. Berstad, E. De Lena, C. Fu, A. Jamali, J.-F. Perez-Calvo, M. Romano, CEMCAP. CO2 capture from cement production, D4.6 CEMCAP Comparative Techno-Economic Analysis of CO2 Capture in Cement Plants, 2019.
[54] K. Evans, The history, challenges, and new developments in the management and use of bauxite residue, J. Sustain. Metall. 2 (2016) 316–331, https://doi.org/10.1007/S40831-016-0060-X/FIGURES/14.
[55] D. Donaldson, Light Metals (2008), https://doi.org/10.1201/9781420011906.sec3.
[56] International Aluminium Institute [IAI], ADDENDUM TO THE LIFE CYCLE INVENTORY DATA AND ENVIRONMENTAL METRICS FOR THE PRIMARY ALUMINIUM INDUSTRY 2015 DATA FINAL, 2018.
[57] M. Strojny, P. Gładysz, D.P. Hanak, W. Nowak, Comparative analysis of CO2 capture technologies using amine absorption and calcium looping integrated with natural gas combined cycle power plant, Energy 284 (2023) 128599, https://doi.org/10.1016/J.ENERGY.2023.128599.
[58] R. Chirone, A. Paulillo, A. Coppola, F. Scala, Carbon capture and utilization via calcium looping, sorption enhanced methanation and green hydrogen: a techno-economic analysis and life cycle assessment study, Fuel 328 (2022) 125255, https://doi.org/10.1016/J.FUEL.2022.125255.
[59] Eurostat - European Commission, Gas prices for household consumers - bi-annual data (from 2007 onwards). https://ec.europa.eu/eurostat/databrowser/view/nrg_pc_202/default/bar?lang=en, 2022. (Accessed 16 January 2023).
[60] M.C. Romano, M. Spinelli, S. Campanari, S. Consonni, G. Cinti, M. Marchi, E. Borgarello, The calcium looping process for low CO2 emission cement and power, Energy Proc. 37 (2013) 7091–7099, https://doi.org/10.1016/J.EGYPRO.2013.06.645.